



Performance Evaluation of Pixel Clustering Approaches for Automatic Detection of Small Bowel Obstruction from Abdominal Radiographs

Kwang Baek Kim* , *Member, KIICE*

Department of Artificial Intelligence, Silla University, Busan 46958, Korea

Abstract

Plain radiographic analysis is the initial imaging modality for suspected small bowel obstruction. Among the many features that affect the diagnosis of small bowel obstruction (SBO), the presence of gas-filled or fluid-filled small bowel loops is the most salient feature that can be automatized by computer vision algorithms. In this study, we compare three frequently applied pixel-clustering algorithms for extracting gas-filled areas without human intervention. In a comparison involving 40 suspected SBO cases, the Possibilistic C-Means and Fuzzy C-Means algorithms exhibited initialization-sensitivity problems and difficulties coping with low intensity contrast, achieving low 72.5% and 85% success rates in extraction. The Adaptive Resonance Theory 2 algorithm is the most suitable algorithm for gas-filled region detection, achieving a 100% success rate on 40 tested images, largely owing to its dynamic control of the number of clusters.

Index Terms: Small Bowel Obstruction (SBO), Adaptive Resonance Theory 2, Fuzzy C Means, Possibilistic C Means, Gas-filled Region

I. INTRODUCTION

Bowel obstruction, also known as intestinal obstruction, is a mechanical or functional obstruction of the intestine that prevents the normal movement of digestion products. Either the small or large bowel may be affected [1]. In the mechanical form of small bowel obstruction (SBO), the proximal gut is distended by swallowed gas and fluid that arises from gastric, small bowel, pancreatic, and biliary secretions. Fluid sequestered within the small bowel is drawn from the circulating blood volume and interstitial spaces, and copious vomiting exacerbates fluid loss and electrolyte depletion. The resulting hypovolemia may be fatal [2]. SBO continues to be a substantial cause of morbidity and mortality, accounting for 12-16% of hospital admissions for the evaluation of

acute abdominal pain in the United States [3]. The etiologies include adhesions (65%), hernias (10%), neoplasms (5%), Crohn's disease (5%), and others (15%) [4].

Most patients suspected of having SBO undergo abdominal radiography largely because it is accurate, readily available, and inexpensive [5,6]. Plain radiography is the initial imaging modality used for the evaluation of patients with suspected bowel obstruction, followed by computed tomography (CT) as the definitive investigation. The accuracy of radiography for the diagnosis of SBO varies from 50 to 86%, according to patient selection and various study design factors [7]. In addition, a weak operator dependency on accuracy was reported [8]. The radiographic findings of SBO include the size of the dilatation (>2.5 cm), stretch sign, multiple air fluid levels, and other factors that are well summa-


Received 29 August 2022, Revised 13 September 2022, Accepted 14 September 2022

*Corresponding Author Kwang Baek Kim (E-mail: gbkim@silla.ac.kr, Tel: +82-51-999-5052)

Department of Artificial Intelligence, Silla University, Busan 46958, Korea

Open Access <https://doi.org/10.56977/jicce.2022.20.3.153>

print ISSN: 2234-8255 online ISSN: 2234-8883

 This is an Open Access article distributed under the terms of the Creative Commons Attribution Non-Commercial License (<http://creativecommons.org/licenses/by-nc/3.0/>) which permits unrestricted non-commercial use, distribution, and reproduction in any medium, provided the original work is properly cited.

Copyright © The Korea Institute of Information and Communication Engineering

rized in [7].

Multi-detector computed tomography (CT) might be the single best imaging tool for suspected SBO. CT has a sensitivity and specificity of 95% for the diagnosis of high-grade SBO, but is less accurate in partial obstruction cases [9]. Furthermore, this modality is expensive, time consuming, and involves high radiation exposure, which is 10 times higher than that associated with abdominal radiography [10]. Thus, plain radiograph analysis is a logical initial imaging modality for suspected small bowel obstruction.

In this study, we evaluate the core image segmentation algorithms that extract the gas-filled region of suspected small bowel obstruction cases using plain radiography. While the diagnosis of SBO from plain radiography should take into account many more factors as summarized in reviews [7], such factors or indices should also be based on a robust and accurate representation of the region or regions of interest (ROI) Among the factors related to diagnosing SBO, the most salient feature is the presence of gas-filled or fluid-filled small bowel loops whose mean air-fluid level width is greater than or equal to 25 mm in upright abdominal radiographs [7, 11]. The presence of a stretch sign, defined as small-bowel gas arrayed as stripes perpendicular to the long axis of the bowel, is also a strong indicator of a predominantly fluid-filled small bowel loop [5].

Furthermore, as discussed in various reports, the sensitivity and specificity of SBO diagnosis vary significantly, and some degree of operator bias has been noted with respect to operator skill and experience [8]; thus, the computer-aided software used in this domain should be as automatic as possible to provide useful information for decision making by field pathologists.

Therefore, we focus on detecting gas-filled areas automatically to avoid any operator effect from SBO-suspected radiography. There are only a few reports analyzing automatic detection of such regions, and the Hough transform and edge detection have been shown to be unsatisfactory in SBO cases [12]. A convolutional neural network (CNN) was applied to the diagnosis of SBO recently [13] but the pilot study is not directly matched to the detecting gas-filled area.

Image segmentation refers to the process of partitioning an image into mutually exclusive regions. It can be considered as the most essential and crucial process for facilitating the delineation, characterization, and visualization of regions of interest in any medical image [14]. Clustering can be defined as the optimal partitioning of a given set of N data points into C subgroups, such that data points belonging to the same group are as similar to each other as possible, whereas data points from two different groups have the maximum difference. Image segmentation can be treated as a clustering problem where the features describing each pixel correspond to a pattern, and each image region corresponds to a cluster [15].

Such pixel clustering algorithms have been successfully applied to detect target organs in input images [14,16-23]. This problem is difficult, especially for medical interpretation, because medical images commonly have poor contrast, different types of noise, and missing or diffuse boundaries [24]. Previous efforts have used pixel clustering to identify a target organ or region covered with brain tumors [14,16], brachial artery detection [17], extraction of rotator cuff tendon tears [18], cervical vertebrae [19], lung cancer [20], inflamed appendix [21], ganglion cyst [22], and for breast image segmentation [23].

In detecting the gas-filled region using abdominal radiography, we compared three frequently used algorithms: Fuzzy C-means (FCM), Possibilistic C-Means (PCM), and Adaptive Resonance Theory (ART) 2, which is the extended version of the original ART to continuous features using the same image set. Each algorithm has advantages and disadvantages and has been successfully applied to some aspects of medical image segmentation problems. With this comparative performance evaluation, we can find the best strategy for SBO detection.

II. PIXEL CLUSTERING ALGORITHMS FOR AUTOMATIC EXTRACTION OF GAS-FILLED REGION

A. Fuzzy C-Means (FCM) Clustering

FCM clustering [25,26] is an unsupervised clustering technique applied to segmenting images into clusters with similar spectral properties. It utilizes the distance between pixels and cluster centers in the spectral domain to compute the membership values of pixels with respect to different clusters. The cost function is minimized by assigning pixels close to the centroid of their cluster with high membership values and low membership values to pixels far from the centroid. The membership function represents the probability that a pixel belongs to a specific cluster. In the FCM algorithm, the probability depends solely on the distance between the pixel and each individual cluster center in the feature domain. The membership function and cluster centers are updated as follows:

Step 1: Initialize the number of clusters c ($2 \leq c < n$), apply an exponential weight m ($1 \leq m < \infty$), membership degree $u(0)$, and error threshold (ϵ).

Step 2: Compute the central vector V_{ij} using Equation (1) for $\{v_i | i = 1, 2, \dots, c\}$.

$$V_{ij} = \frac{\sum_{k=1}^n (U_{ik})^m x_{kj}}{\sum_{k=1}^n (U_{ik})^m} \quad (1)$$

Here, X is the input pattern, i is the cluster index, and j is the pattern-node index. where k is the pattern index, n is the

number of patterns, and U is the membership function.

Step 3: Define the FCM cost function J (Eq. (2)), where d_{ik} is the distance between the k -th pattern x_k and the central vector of the i -th cluster, and u_{ik} is the membership degree of x_k among the patterns in the i -th cluster.

$$J(u_{ik}, v_i) = \sum_{i=1}^c \sum_{k=1}^n (u_{ik})^m (d_{ik})^2 \quad (2)$$

To minimize J , d_{ik} and membership function U are defined in Equations (3) and (4), respectively.

$$d_{ik} = \sqrt{\sum_{j=1}^l (x_{kj} - v_{ij})^2} \quad (3)$$

$$U_{ik} = 1 / \sum_{i=1}^c \left(\frac{d_{ik}}{d_{ik}} \right)^{\frac{2}{m-1}} \quad (4)$$

In the equations, l is the number of pattern nodes, and C is the number of clusters.

Step 4: Compute the difference between the new and previous membership degrees ($U_{ik}(r+1) - U_{ik}(r)$). If the difference is larger than a pre-defined error threshold (ϵ), then return to Step 2; otherwise, stop the algorithm.

B. Possibilistic C-Means (PCM) [27]

In the standard FCM technique, a noisy pixel can be incorrectly classified because of its abnormal feature data [27]. Possibilistic C-means (PCM) clustering is another unsupervised clustering method where the component generated by PCM corresponds to a dense region in the dataset. PCM is known to be more robust to noisy data. The PCM membership degree refers to the degree of ‘typicality’ between the data and clusters [28].

PCM is based on the relaxation of the probabilistic constraint in order to interpret the membership function or degree of typicality based on a possibilistic sense.

Then $U_p = (u_{ij})$ is considered a possibilistic cluster partition of X if

$$\sum_{j=1}^n u_{ij} > 0, \forall i \in \{1, \dots, c\}, \quad (5)$$

where $u_{ij} \in [0, 1]$ is interpreted as the degree of typicality of datum x_j to cluster i , and u_{ij} for x_j indicates the possibility of x_j being a member of the corresponding cluster.

The objective function in PCM clustering can be calculated as

$$J_m(L, U) = \sum_{i=1}^c \sum_{j=1}^n (u_{ij})^m d_{ij}^2 + \sum_{i=1}^c n_i \sum_{j=1}^n (1 - u_{ij}^m), \quad (6)$$

where n_i denotes the average distance between points in the same group and d_{ij} is the distance between x_i and x_j . The first term of Eq. (6) attempts to minimize the distance between

the data point and the cluster center, and the second term is a penalty term used to avoid obtaining a trivial solution.

The update formula for the membership degree is defined as

$$u_{ij} = \frac{1}{1 + \left(\frac{d_{ij}}{n_i} \right)^{\frac{2}{m-1}}}, \quad (7)$$

where n_i determines the distance at which the membership degree in the cluster is 0.5. Thus, it represents the relative importance of the second term with respect to the first term in the objective function (Equation (6)), and is typically estimated using Equation (8) as follows:

$$n_i = K \times \frac{\sum_{j=1}^n u_{ij}^m d_{ij}^2}{\sum_{j=1}^n u_{ij}^m}, \quad (8)$$

where $K = 1$ in this study.

However, PCM has a disadvantage in that it requires good initialization to obtain good results [29]. To classify a data point, the cluster centroid must be closest to the data point (by membership), and to estimate the centroids, the typicality needs to alleviate the undesirable effect of outliers. Therefore, it is possible that PCM will stop even if the number of clusters processed is less than the actual pre-set number of clusters.

C. Adaptive Resonance Theory (ART) 2

For an arbitrary input pattern, ART2 offers a solution to the plasticity-stability problem without suffering from the local minima problem [30]. The general characteristics of ART2 were extended to cover continuous features not available in the original ART, and ART2 can be summarized as follows:

1. An unsupervised real time learning algorithm that does not use a target value.
2. It creates a new cluster or merges existing clusters according to the similarity between an input pattern and the current set of clusters.
3. It can learn from analog or grey-level component input vectors.

The detailed ART2 behavior is summarized as shown in Fig. 1.

The output vector O_j is computed by Equation (9), and the winner node is determined to have the minimum output, as indicated by Equation (10).

$$O_j = \frac{1}{N} \sum_{i=0}^{N-1} |x_i - w_{ji}(t)| \quad (9)$$

$$O_{j^*} = \text{Min}(O_j) \quad (10)$$

In the equations, N denotes the number of inputs and $w_{ji}(t)$ denotes the connection weight between the input layer and the cluster layer.

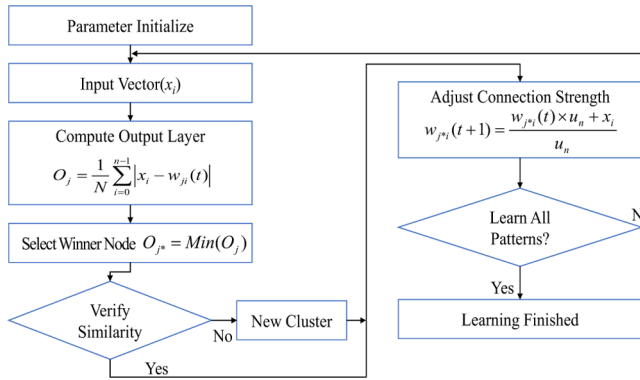


Fig. 1. ART2 Clustering Process.

To control the number of clusters dynamically, we verify the similarity between the winner node and the input pattern using Equation (11), where ρ is the value of the vigilance parameter ($0 \leq \rho \leq 0.5$). If the output of the winner node is less than ρ , then that node is included within the known cluster, and the weight strengths are adjusted using Equation (12). Otherwise, the winner node starts a new cluster.

$$O_{j^*} < \rho \tag{11}$$

$$w_{j^*i}(t+1) = \frac{w_{j^*i}(t) \times u_n + x_i}{u_n} \tag{12}$$

Here, u_n denotes the number of updated patterns in the cluster.

Pixels are then clustered using the ART2 principles. The similarity between the winner node and existing clusters is used to extract the object’s form based on the brightness value.

III. Experiment

The proposed method is implemented by C# under the Visual Studio 2017 environment on an IBM PC with an Intel Core(TM) i7-6700HQ CPU @ 2.60GHz and 8 GB RAM. Forty (40) X-ray images containing suspected SBO with a size of 1208×1502 were used in this experiment. All 40 images were obtained from Gupo Sungsim Hospital, Busan, Korea.

All input images underwent the same preprocessing and object modelling procedures, except for the pixel clustering phases conducted by the three algorithms evaluated. For FCM and PCM, the number of clusters should be initialized before processing; thus, we set the number to 4 for PCM and

6 for FCM, which were selected based on pilot tests conducted using eight images. ART2 has dynamic control of cluster formation; thus, there was no specific initialization. On average, it used 5.8 clusters (minimum 3, maximum 7), as shown in Table 1. The vigilance parameter for ART2 was 0.08 throughout the experiment. The extraction results were verified by radiologists in the hospital, and they decided whether the extraction by a vision algorithm was satisfactory. The experimental results are summarized in Table 1.

As shown in Table 1, drastic differences are present among the three compared pixel clustering algorithms regarding the correct extraction of gas-filled areas. ART2 achieved perfect accuracy, whereas the other two algorithms were not quite as successful. A retrospective analysis is needed to determine why such results were obtained in this experiment.

Table 1. Performance Comparison of Gas-filled Area Extraction Algorithms

Taxonomy	ART2	FCM	PCM
Success	40	34	29
Fail	0	6	11
Rate (%)	100.0 %	85.0 %	72.5 %
# of Clusters	5.8 (Avg.)	6	4

In Fig. 2, we show a typical case in which the PCM fails, but the other two algorithms are successful. Although both FCM and PCM are used for segmentation, there are some differences between these two algorithms. In FCM, membership degree refers to the degree of sharing (belongingness) between the data and clusters. On the other hand, the PCM membership degree refers to the degree of ‘typicality’ between data and clusters. The membership degree of a data point to a cluster is independent of its membership to other clusters.

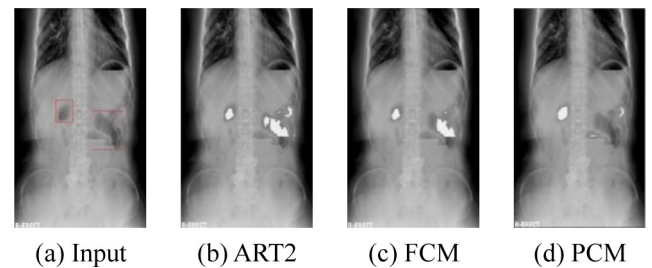


Fig. 2. Case when PCM Fails.

The “fuzzifier” interprets different meanings in FCM and PCM. In FCM, ‘increasing’ indicates the increased sharing of points among clusters, whereas this means an increased possibility of all points in the dataset completely belonging to a given cluster in PCM. In a noisy environment, PCM is known to be less sensitive than FCM; however, PCM may lead to all cluster centers being identical. That is, PCM also

has a stability problem if it is not properly initialized, as shown in Fig. 2. In retrospect, ART2 formed six clusters (the same as FCM), but PCM was initialized as having only four clusters. Thus static initialization is critical for problems in this domain, where the form of the target objects may have various patterns such that the number of clusters necessary can vary over a relatively wide range.

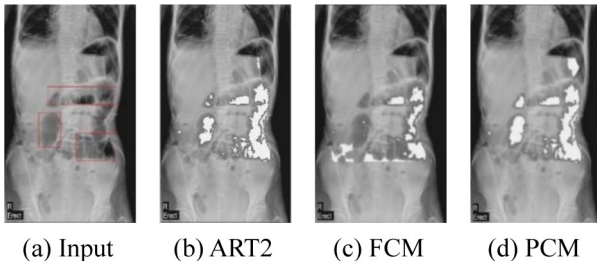


Fig. 3. Case when FCM Fails.

In contrast, only FCM failed in the case shown in Fig. 3. In this case, FCM shows its weakness with respect to noise, and a problem arises when a data point has the same membership value for two or more clusters. In this case, FCM cannot distinguish between a moderately atypical member and an extremely atypical member. This is largely due to FCM's constraint that the sum of the membership degree should be exactly equal to 1, which may cause problems in normalizing the distance between clusters. PCM was better in this case because it relaxes this constraint, where the membership degree reflects the typicality, and PCM is thus more tolerant to noise than FCM.

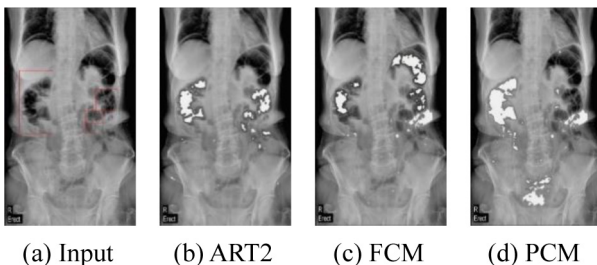


Fig. 4. Case when only ART2 succeeds.

Unfortunately, there can be cases such as the one depicted in Fig. 4, where a significant density difference among pixels is present in the ROI. In such cases, only ART2 achieved successful extractions. Both FCM and PCM use static initialization of the number of clusters, and are thus less flexible during clustering. In FCM, because the sum of the membership degree must equal 1 and only a single winning node is selected based on the membership function degree, a wide variance in pixel density can cause misclassifications, as shown in Fig. 4(c). For the PCM case, as shown in Fig. 4(d),

because of the static initialization of the number of clusters and the difficulty in computing the average distance among intra-cluster points when significant density differences are present, the extraction of the gas-filled area does not always match the actual shape. The success of ART2 in this domain can be attributed to its flexibility in cluster formation and its membership degree interpretation with respect to the related clusters.

IV. CONCLUSIONS

In this study, we conducted an experiment to compare three frequently used pixel clustering algorithms used to extract gas-filled areas from radiographs of patients suspected of suffering from SBO. In diagnosing SBO, this feature is not the only one used to determine the medical condition, but it is the most salient feature in clinical situations. The three algorithms considered were FCM, PCM, and ART2.

In the comparison using the 40 suspected SBO cases in our experiment, PCM was the least effective because of its defuzzification based on the probability distribution and the static initialization of the number of clusters. Typically, the input image does not have sufficient intensity contrast between the target area and the surrounding background; thus, PCM is the most sensitive to extract and form an object (gas-filled area). Therefore, it tends to use fewer clusters, such that the form of the object is different than the actual object in many complex-obstruction shape cases. A similar problem occurs for FCM in that the static initialization of the number of clusters limits the capability of the algorithm to reproduce the target object using membership classifications. ART2, on the other hand, exhibits no difficulties in extracting gas-filled areas because of its dynamic control of the number of clusters.

ACKNOWLEDGMENTS

Following are results of a study on the “Leaders in INdustry-university Cooperation 3.0” Project, supported by the Ministry of Education and National Research Foundation of Korea.

REFERENCES

- [1] R. M. Gore, R. I. Silvers, K. H. Thakrar, D. R. Wenzke, U. K. Mehta, G. M. Newmark, and J. W. Berlin, “Bowel obstruction,” *Radiologic Clinics of North America*, vol. 53, no. 6, pp. 1225-1240, Nov. 2015. DOI: 10.1016/j.rcl.2015.06.008.
- [2] S. B. Williams, J. Greenspon, H. A. Young, and B. A. Orkin, “Small bowel obstruction: Conservative vs. surgical management,” *Diseases*

- of the Colon & Rectum, vol. 48, no. 6, pp. 1140-1146, Apr. 2005. DOI: 10.1007/s10350-004-0882-7.
- [3] S. Nicolaou, B. Kai, S. Ho, J. Su, and K. Ahamed, "Imaging of acute small-bowel obstruction," *American Journal of Roentgenology*, vol. 185, no. 4, pp. 1036-1044, Oct. 2005. DOI: 10.2214/AJR.04.0815.
- [4] S. R. Reddy and M. S. Cappell, "A systematic review of the clinical presentation, diagnosis, and treatment of small bowel obstruction," *Current Gastroenterology Reports*, vol. 19, no. 6, pp. 28-41, Apr. 2017. DOI: 10.1007/s11894-017-0566-9.
- [5] J. C. Lappas, B. L. Reyes, and D. D. Maglinte, "Abdominal radiography findings in small-bowel obstruction: Relevance to triage for additional diagnostic imaging," *American Journal of Roentgenology*, vol. 176, no. 1, pp. 167-174, Jan. 2001. DOI: 10.2214/ajr.176.1.1760167.
- [6] D. D. T. Maglinte, D. E. Heitkamp, T. J. Howard, F. M. Kelvin, and J. C. Lappas, "Current concepts in imaging of small bowel obstruction," *Radiologic Clinics North America*, vol. 41, no. 2, pp. 263-283, Mar. 2003. DOI: 10.1016/s0033-8389(02)00114-8.
- [7] E. K. Paulson and W. M. Thompson, "Review of small-bowel obstruction: The diagnosis and when to worry," *Radiology*, vol. 275, no. 2, pp. 332-342, May. 2015. DOI: 10.1148/radiol.15131519.
- [8] W. M. Thompson, R. K. Kilani, B. B. Smith, J. Thomas, T. A. Jaffe, D. M. Delong, and E. K. Paulson, "Accuracy of abdominal radiography in acute small-bowel obstruction: Does reviewer experience matter?," *American Journal of Roentgenology*, vol. 188, no. 3, pp. W233-W238, Mar. 2007. DOI: 10.2214/AJR.06.0817.
- [9] R. B. Jeffrey, *Small bowel obstruction. Diagnostic imaging: abdomen*, 2nd ed. Salt Lake City: UT, USA, pp. 44-47, 2010.
- [10] S. Suri, S. Gupta, P. J. Sudhakar, N. K. Venkataramu, B. Sood, and J. D. Wig, "Comparative evaluation of plain films, ultrasound and CT in the diagnosis of intestinal obstruction," *Acta radiologica*, vol. 40, no. 4, pp. 422-428, Jan. 1999. DOI: 10.3109/02841859909177758.
- [11] R. M. Gore and M. S. Levine, *Textbook of gastrointestinal radiology*, 3rd ed. Philadelphia, PA: Elsevier, 2008.
- [12] H. I. Lee, B. C. Kim, H. W. Kim, S. U. Park, and K. B. Kim, "Ileus detection by using edge information and hough transform," in *Proceedings of Fall Conference of Korea Institute of Information and Communication Engineering*, vol. 21, no. 2, pp. 488-490, Oct. 2017.
- [13] P. M. Cheng, T. K. Tejura, K. N. Tran, and G. Whang, "Detection of high-grade small bowel obstruction on conventional radiography with convolutional neural networks," *Abdominal Radiology*, vol. 43, no. 5, pp. 1120-1127, Aug. 2018. DOI: 10.1007/s00261-017-1294-1.
- [14] E. Abdel-Maksoud, M. Elmogy, and R. Al-Awadi, "Brain tumor segmentation based on a hybrid clustering technique," *Egyptian Informatics Journal*, vol. 16, no. 1, pp. 71-81, Mar. 2015. DOI: 10.1016/j.eij.2015.01.003.
- [15] A. K. Jain, M. N. Murty, and P. J. Flynn, "Data clustering: A review," *ACM computing surveys (CSUR)*, vol. 31, no. 3, pp. 264-323, Sep. 1999. DOI: 10.1145/331499.331504.
- [16] V. P. Ananthi, P. Balasubramaniam, and T. Kalaiselvi, "A new fuzzy clustering algorithm for the segmentation of brain tumor," *Soft Computing*, vol. 20, no. 12, pp. 4859-4879, Jul. 2016. DOI: 10.1007/s00500-015-1775-5.
- [17] J. Park, D. H. Song, H. Nho, H. M. Choi, K. A. Kim, H. J. Park, and K. B. Kim, "Automatic segmentation of brachial artery based on fuzzy C-means pixel clustering from ultrasound images," *International Journal of Electrical and Computer Engineering*, vol. 8, no. 2, pp. 638-643, Apr. 2018. DOI: 10.11591/ijece.v8i2.pp638-643.
- [18] K. B. Kim, Y. S. Song, H. J. Park, D. H. Song, and B. K. Choi, "A fuzzy C-means quantization based automatic extraction of rotator cuff tendon tears from ultrasound images," *Journal of Intelligent & Fuzzy Systems*, vol. 35, no. 1, pp. 149-158, Jul. 2018. DOI: 10.3233/JIFS-169576.
- [19] H. J. Lee, D. H. Song, and K. B. Kim, "Effective computer-assisted automatic cervical vertebrae extraction with rehabilitative ultrasound imaging by using K-means clustering," *International Journal of Electrical and Computer Engineering*, vol. 6, no. 6, pp. 2810-2817, Dec. 2016. DOI: 10.11591/ijece.v6i6.13268.
- [20] M. A. Hussain, T. M. Ansari, P. S. Gawas, and N. N. Chowdhury, "Lung cancer detection using artificial neural network & fuzzy clustering," *International Journal of Advanced Research in Computer and Communication Engineering*, vol. 4, no. 3, pp. 360-363, Mar. 2015. DOI: 10.17148/IJARCC.2015.4386.
- [21] K. B. Kim, D. H. Song, and H. J. Park, "Automatic extraction of appendix from ultrasonography with self-organizing map and shape-brightness pattern learning," *BioMed Research International*, Apr. 2016. DOI: 10.1155/2016/5206268.
- [22] Suryadibrata and K. B. Kim, "Ganglion cyst region extraction from ultrasound images using possibilistic C-means clustering method," *Journal of information and communication convergence engineering*, vol. 15, no. 1, pp. 49-52, Mar. 2017. DOI: 10.6109/jicce.2017.15.1.49.
- [23] H. M. Moftah, A. T. Azar, E. T. Al-Shammari, N. I. Ghali, A. E. Hassanien, and M. Shoman, "Adaptive k-means clustering algorithm for MR breast image segmentation," *Neural Computing and Applications*, vol. 24, no. 7-8, pp. 1917-1928, Jun. 2014. DOI: 10.1007/s00521-013-1437-4.
- [24] A. Chien, B. Dong, and Z. Shen, "Frame-based segmentation for medical images," *Communications in Mathematical Sciences*, vol. 9, no. 2, pp. 551-559, Dec. 2011. DOI: 10.4310/CMS.2011.v9.n2.a10.
- [25] M. S. Yang, Y. J. Hu, K. C. Lin, C. C. Lin, "Segmentation techniques for tissue differentiation in MRI of ophthalmology using fuzzy clustering algorithms," *Magnetic Resonance Imaging*, vol. 20, no. 2, pp. 173-179, Feb. 2002. DOI: 10.1016/S0730-725X(02)00477-0.
- [26] K. B. Kim, H. J. Lee, D. H. Song, and Y. W. Woo, "Extracting fascia and analysis of muscles from ultrasound images with FCM-based quantization technology," *Neural Network World*, vol. 20, no. 3, pp. 405-416, 2010.
- [27] K. S. Chuang, H. L. Tzeng, S. Chen, J. Wu, and T. J. Chen, "Fuzzy c-means clustering with spatial information for image segmentation," *Computerized Medical Imaging and Graphics*, vol. 30, no. 1, pp. 9-15, Jan. 2006. DOI: 10.1016/j.compmedimag.2005.10.001.
- [28] H. Yu, J. Fan, and R. Lan, "Suppressed possibilistic c-means clustering algorithm," *Applied Soft Computing*, vol. 80, pp. 845-872, Jul. 2019. DOI: 10.1016/j.asoc.2019.02.027.
- [29] W. Zeng, Y. Liu, H. Cui, R. Ma, and Z. Xub, "Interval possibilistic C-means algorithm and its application in image segmentation," *Information Sciences*, vol. 612, pp. 464-480, Oct. 2022. DOI: 10.1016/j.ins.2022.08.082.
- [30] J. Park, D. H. Song, S. -S. Han, S. J. Lee, and K. B. Kim, "Automatic extraction of soft tissue tumor from ultrasonography using ART2 based intelligent image analysis," *Current Medical Imaging*, vol. 13, no. 4, pp. 447-453, Nov. 2017. DOI: 10.2174/1573405613666170504153002.



Kwang Baek Kim

Kwang Baek Kim received his M.S. and Ph.D. degrees from the Department of Computer Science, Pusan National University, Busan, Korea in 1993 and 1999, respectively. From 1997-2020, he was a professor at the Department of Computer Engineering, Silla University, Korea. From 2021 to the present, he is a professor at the Department of Artificial Intelligence, Silla University, Korea. He is currently an associate editor for Journal of Intelligence and Information Systems. His research interests include fuzzy clustering and applications, machine learning, and image processing.